Organic & Biomolecular Chemistry

Accepted Manuscript

This article can be cited before page numbers have been issued, to do this please use: S. Zhang, X. Wu, Y. Lin, S. Wu, G. Tang, L. Gong and A. Abdukader, *Org. Biomol. Chem.*, 2026, DOI: 10.1039/D6OB00666C.

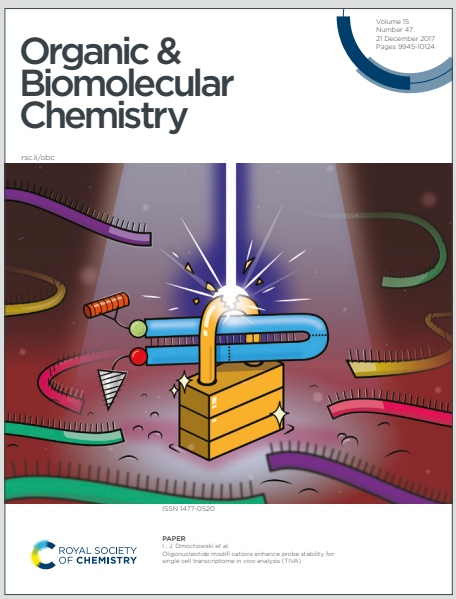

ROYAL SOCIETY OF CHEMISTRY

rsc.li/obc

View Article Online
DOI: 10.1039/D6OB00666C

ARTIC

Transition-metal-free three-component synthesis of α-tertiary trifluoromethyl phosphonates from CF_3 diazo compounds

Received 00th January 20xx,
Accepted 00th January 20xx

DOI: 10.1039/x0xx00000x

Shuangming Zhang,[a,b] Xianda Wu,[b] Yu-Mei Lin,[b,] Shaofeng Wu,[a] Guo Tang,[a,b,]* Lei Gong,[a, b,]* Ablimit Abdukader[a,]*

α-Trifluoromethylated phosphonates are highly valued in medicinal chemistry and functional materials, yet their efficient synthesis remains challenging. Herein, we report a practical, transition-metal-free strategy for the rapid assembly of this important class of scaffolds via a one-pot, three-component reaction, using α-trifluoromethyl diazo compounds as key precursors together with readily accessible H-phosphites and benzyl bromides or alkyl halides. This mild reaction proceeds through a base-promoted, ordered nucleophilic attack sequence, enabling the simultaneous formation of C–C and C–P bonds and affording products bearing congested, fully substituted carbon centers in high yields (up to 98%). The selected products were predicted to have favorable pharmacokinetic properties based on in silico ADME analysis. This work provides a general synthetic route to α-trifluoromethylated phosphonates and highlights their broad application prospects in drug discovery and functional materials development.

Introduction

Compounds bearing phosphonate motifs have found widespread utility in pharmaceutical development, agrochemical research, and materials science.[1–3] Incorporation of a compact and highly electronegative trifluoromethyl (CF_3) group into phosphonate frameworks can profoundly modulate their physicochemical and biological properties, including fine-tuned lipophilicity, enhanced membrane permeability, and improved pharmacokinetic profiles.[4–8] In particular, α-trifluoromethylated phosphonates, wherein both a CF_3 group and a phosphonate unit reside on the same carbon atom, exhibit a distinctly modified steric and electronic environment (Fig. 1A).[9–11] This structural perturbation, arising from the strong electron-withdrawing effect of the CF_3 moiety, can significantly influence biological activity and has therefore attracted increasing research interest.[12]

Existing synthetic routes to α-trifluoromethylated phosphonates, particularly those bearing congested, fully substituted carbon centers, have primarily relied on two strategies: phosphonylation of preformed CF_3-containing building blocks or direct nucleophilic or electrophilic trifluoromethylation of phosphonates.[13–19] For example, Feng et al. described an enantioselective hydrophosphonylation of trifluoromethyl ketones using a chiral hydrogenated tridentate Schiff base aluminum(III) complex, affording α-hydroxy trifluoromethyl phosphonates (Fig. 1B, eq 1, 8 examples).[16] Qing and colleagues achieved the synthesis of α-trifluoromethyl-β-keto phosphonates through the reaction of β-keto phosphonates with Togni reagent in the presence of sodium tert-butoxide and hexamethylphosphoramide (HMPA) (Fig. 1B, eq 2, 12 examples).[17] Ohshima and co-workers developed a direct enantioselective hydrophosphonylation of trifluoromethyl ketimines catalyzed by chiral bifunctional squaramide organocatalysts, providing access to α-amino trifluoromethyl phosphonates (Fig. 1B, eq 3, 10 examples).[18] Despite these advances, current methodologies are often constrained by a limited substrate scope and remain largely restricted to specific classes of starting materials. Moreover, a persistent challenge lies in the difficulty of diversifying the two remaining substituents on the congested, fully substituted carbon center. Collectively, these limitations have hampered the broader application of such scaffolds in drug discovery and functional materials development.

Diazo compounds, known for their high reactivity, have played an indispensable role in the formation of carbon–carbon and carbon–heteroatom bonds.[20–30] Inspired by advances in fluorine and phosphorus chemistry[31–34] and our ongoing interest in sustainable synthesis[35–38], we herein describe a practical one-pot, three-component reaction using α-trifluoromethyl diazo compounds as key precursors, in combination with readily available H-phosphites and benzyl bromides or alkyl halides, for the efficient synthesis of diverse α-trifluoromethylated phosphonate derivatives. This metal-free protocol allows for the simultaneous construction of C–C and C–P bonds, thereby installing the CF_3 and phosphonate groups onto a sterically congested, fully substituted carbon center in a single step. The method accommodates a broad range of electronically and sterically diverse H-phosphites as well as benzyl bromides or alkyl halides, delivering the target products in moderate to excellent yields (up to 98%) over 41 examples. In silico ADME (absorption,

[a] State Key Laboratory of Chemistry and Utilization of Carbon Based Energy Resources, College of Chemistry, Xinjiang University, Urumqi, 830017, China.
E-mail: ablimit1970@126.com ; wusf@xju.edu.cn.
[b] Key Laboratory of Chemical Biology of Fujian Province, College of Chemistry and Chemical Engineering, Xiamen University, Xiamen, Fujian 361005, China.
E-mail: gongl@xmu.edu.cn; linyum@xmu.edu.cn; t12g21@xmu.edu.cn.

distribution, metabolism, and excretion) predictions indicate that selected compounds exhibit favorable pharmacokinetic characteristics, including good oral bioavailability, blood–brain barrier (BBB) permeability potential, and a low risk of P-glycoprotein (P-gp) efflux. This underscores their potential for applications in drug development and materials science.[39]

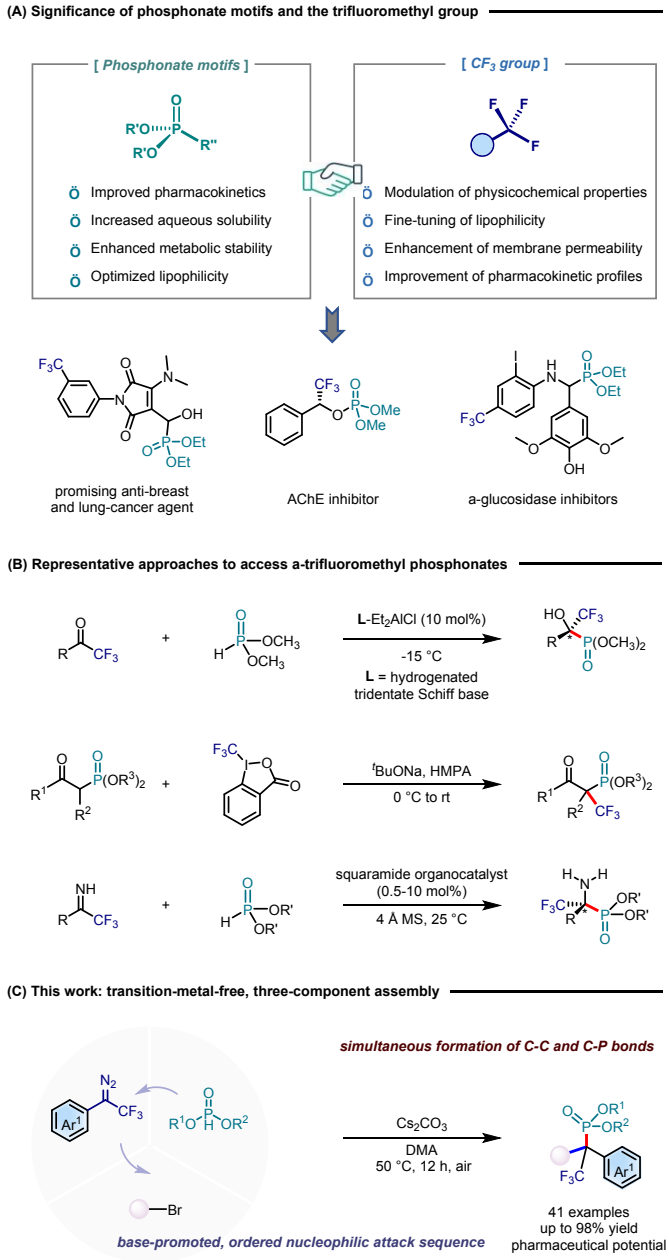

Fig. 1. Overview of this study.

Results and discussion

We began by optimizing the reaction conditions using (1-diazo-2,2,2-trifluoroethyl)benzene (**1a**), diethyl H-phosphite (**2a**), and benzyl bromide (**3a**) as model substrates (Table 1). Initial screening showed that employing Cs_2CO_3 as the base in *N,N*-dimethylacetamide (DMA) at 50 °C for 12 h delivered the desired product **4** in 95% yield (entry 1). Replacing Cs_2CO_3 with K_2CO_3 led to a diminished yield of 84% (entry 2), while other strong bases such as EtONa, $(CH_3)_3COK$, and 1,5,7-triazabicyclo[4.4.0]dec-5-ene (TBD) failed to promote the reaction (entries 3–6). A survey of solvents revealed that DMA was uniquely effective (entries 7–12); solvents such as dichloroethane (DCE), toluene, tetrahydrofuran (THF), and CH_3OH gave no product (entries 7–10), and both acetone and CH_3CN afforded significantly lower yields than DMA (entries 11 and 12). Further investigation showed that reducing the reaction time to 6 h decreased the yield to 72% (entry 13). Temperature also proved critical: performing the reaction at 25 °C under otherwise identical conditions resulted in only 26% yield (entry 15). These experiments established the optimal conditions as Cs_2CO_3 in DMA at 50 °C for 12 h, which were used for subsequent substrate exploration.

Table 1 Optimization of the reaction conditions[a]

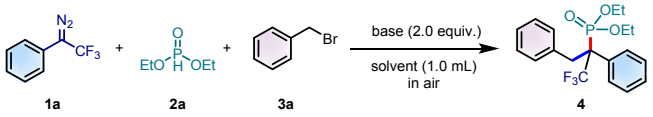

Entry	Base	Solvent	Time (h)	Temp (°C)	Yield (%)[b]
1	Cs_2CO_3	DMA	12	50	95
2	K_2CO_3	DMA	12	50	84
3	K_3PO_4	DMA	12	50	Trace
4	EtONa	DMA	12	50	N.R.
5	$(CH_3)_3COK$	DMA	12	50	N.R.
6	TBD	DMA	12	50	N.R.
7	Cs_2CO_3	DCE	12	50	N.R.
8	Cs_2CO_3	Toluene	12	50	N.R.
9	Cs_2CO_3	THF	12	50	N.R.
10	Cs_2CO_3	CH_3OH	12	50	Trace
11	Cs_2CO_3	Acetone	12	50	19
12	Cs_2CO_3	CH_3CN	12	50	42
13	Cs_2CO_3	DMA	6	50	72
14	Cs_2CO_3	DMA	9	50	85
15	Cs_2CO_3	DMA	12	25	26

[a] Reaction conditions: **1a** (0.10 mmol), **2a** (0.20 mmol), **3a** (0.20 mmol), base (0.20 mmol), solvent (1.0 mL), in air.[b] Isolated yield. N.R., no reaction.

With the optimized conditions in hand, the substrate scope of this transformation was explored (Fig. 2). The study began with an evaluation of α-trifluoromethyl diazo compounds. Substrates

DOI: 10.1039/D6OB00666C

bearing electron-rich arenes, such as those with *para*-methyl, *meta*-methyl, *para*-isopropyl, *para*-*tert*-butyl, *para*-phenyl, and *para*-methoxy substituents (**5–10**), underwent smooth conversion to afford the corresponding products in moderate to good yields of 52–71%. Electron-deficient arenes, including halogenated derivatives (**11–12**), also proved to be competent substrates, delivering the desired products in 50–56% yield. However, α-trifluoromethyl diazo compounds containing strong electron-withdrawing groups, such as ester or nitro moieties, as well as those bearing 3,5-dichloro-substituted aryl rings, were ineffective under the standard conditions.

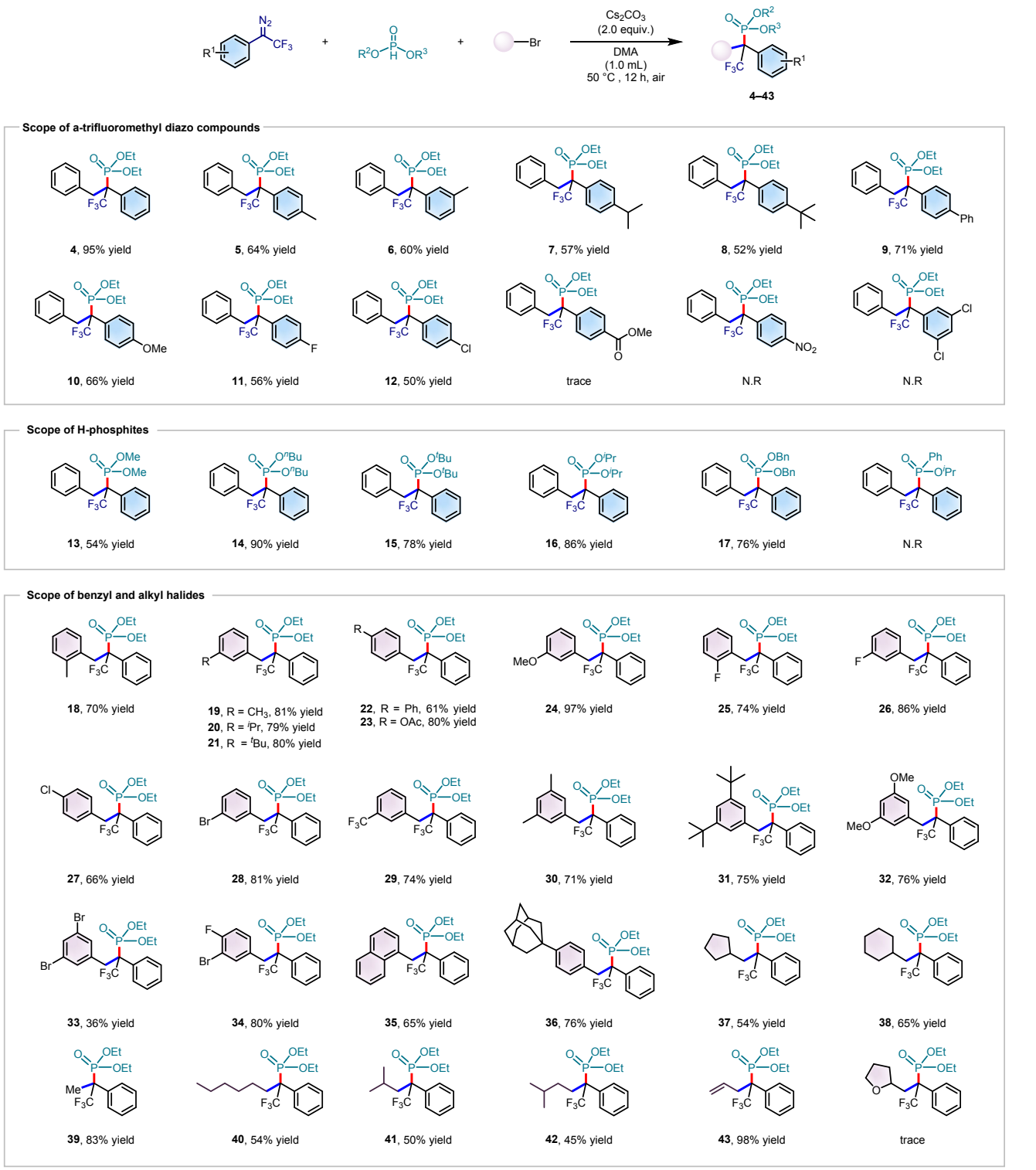

Fig. 2. Substrate scope for the transition-metal-free, three-component reaction. Reaction conditions: **1a** (0.10 mmol), **2a** (0.20 mmol), **3a** (0.20 mmol), base (0.20 mmol), solvent (1.0 mL), in air.

View Article Online
DOI: 10.1039/D6OB00686C

Next, the applicability of various H-phosphites was examined. A range of H-phosphites, including dimethyl H-phosphite (**13**), di-*n*-butyl H-phosphite (**14**), di-*tert*-butyl H-phosphite (**15**), diisopropyl H-phosphite (**16**), and dibenzyl H-phosphite (**17**), all participated efficiently in the reaction. The corresponding products were obtained in yields ranging from 54–90%, highlighting the flexibility for structural modification at the phosphonate group.

Subsequently, the substrate scope of bromides was investigated. Benzyl bromides bearing electron-donating groups, such as *ortho*-methyl (**18**), *meta*-methyl (**19**), *meta*-isopropyl (**20**), or *meta*-*tert*-butyl (**21**) substituents, all reacted smoothly to afford the desired products in good yields. Similarly, substrates bearing *para*-phenyl (**22**), *para*-acetoxy (**23**), or *meta*-methoxy (**24**) groups underwent clean conversion, providing the target compounds in 61–97% yield. Benzyl bromides bearing electron-withdrawing groups also exhibited good tolerance, including halogen-substituted derivatives at the *ortho*, *meta*, or *para* positions (**25–28**) and the *meta*-trifluoromethyl-substituted substrate (**29**). Furthermore, disubstituted benzyl bromides bearing either electron-donating groups (**30–32**) or electron-withdrawing groups (**33–34**) all reacted efficiently under the standard conditions, affording the corresponding products in moderate to excellent yields. Naphthalen-1-ylmethyl bromide (**35**) and *para*-adamantyl benzyl bromide (**36**) were also found to be viable substrates, with isolated yields of 65–76%.

To further assess the generality of this method, the substrate scope was extended to other alkyl halides. Cyclic systems, such as (bromomethyl)cyclopentane (**37**) and (bromomethyl)cyclohexane (**38**), as well as acyclic analogues—including iodomethane (**39**), linear 1-bromohexane (**40**), branched 1-bromo-2-methylpropane (**41**) and 1-bromo-3-methylbutane (**42**), and allyl bromide (**43**)—all participated effectively. These reactions proceeded smoothly, furnishing the corresponding products in moderate to good yields. Collectively, these results demonstrate the broad applicability of this protocol to a diverse array of alkyl halides.

To gain insight into the reaction mechanism, several control experiments were conducted (Fig. 3). Heating **1a** and **2a** with Cs_2CO_3 (1.0 equiv.) delivered diethyl (2,2,2-trifluoro-1-phenylethyl)phosphonate (**44**) in 99% yield; subsequent treatment of **44** with **3a** under identical conditions afforded the final product **4** in 98% yield. In contrast, when **2a** and **3a** were combined with Cs_2CO_3 (1.0 equiv.), diethyl benzylphosphonate (**45**) was isolated in 26% yield; however, this intermediate failed to react further upon the addition of **1a**. These outcomes point to a base-promoted, ordered reaction sequence. To evaluate the potential involvement of radical intermediates, the reaction was carried out in the presence of 2,2,6,6-tetramethylpiperidinooxy (TEMPO, 2.5 equiv.) as a radical scavenger (Fig. 3B). The absence of notable inhibition argues against a radical pathway.

On the basis of these results, a plausible mechanism is proposed (Fig. 3C). The transformation is initiated by the deprotonation of H-phosphite **2a** with Cs_2CO_3 to generate the phosphite anion **INT-I**. This intermediate then undergoes nucleophilic addition to diazo compound **1a**, forming **INT-II**. Subsequent extrusion of dinitrogen from **INT-II** gives the anionic species **INT-III**, which engages in a nucleophilic substitution with benzyl bromide **3a** to deliver the final product **4**. The high efficiency of this transformation is attributed to the sequential and ordered nature of these nucleophilic attack events. The final substitution step is sensitive to electronic and steric effects. Strong electron-withdrawing groups on the diazo compound diminish the nucleophilicity of **INT-III**, retarding the reaction. For the alkyl halides, electron-donating groups (**41**, **42**) lower electrophilicity, while steric hindrance (**46**) physically impedes the attack by **INT-III**. These observations confirm that the high efficiency of the standard reaction with **3a** relies on the favourable electronic and steric environment required for this sequential nucleophilic mechanism.

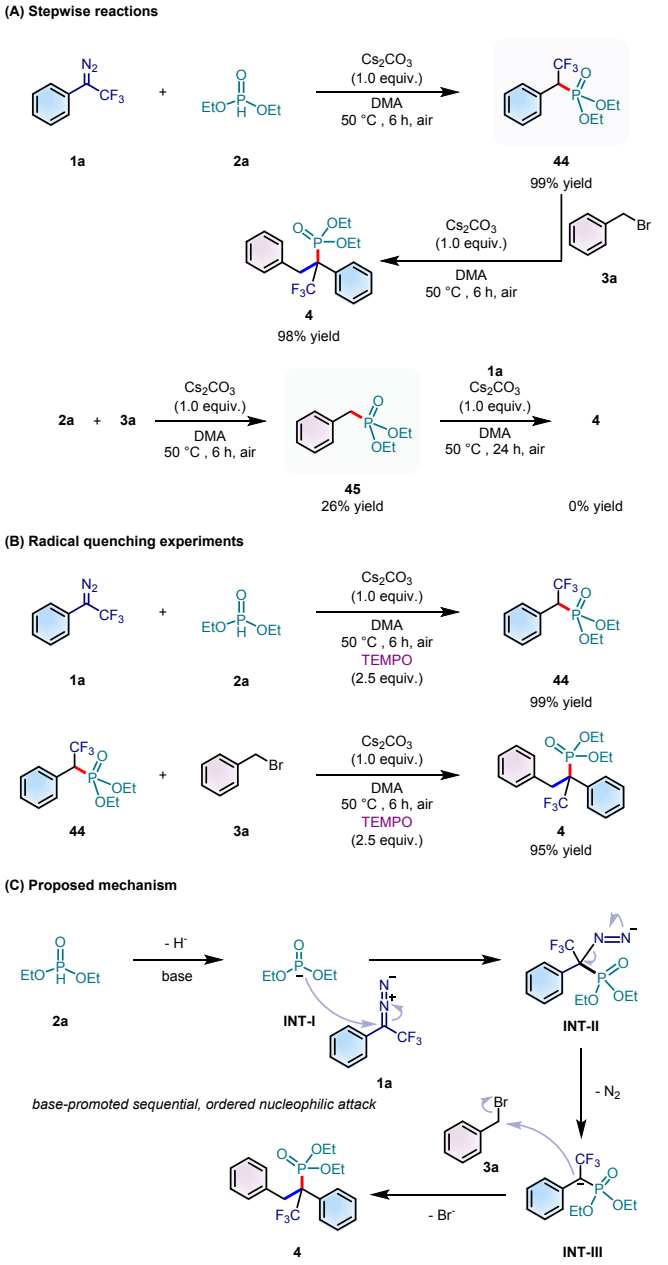

Fig. 3. Mechanistic studies.

View Article Online
DOI: 10.1039/D6OB00666C

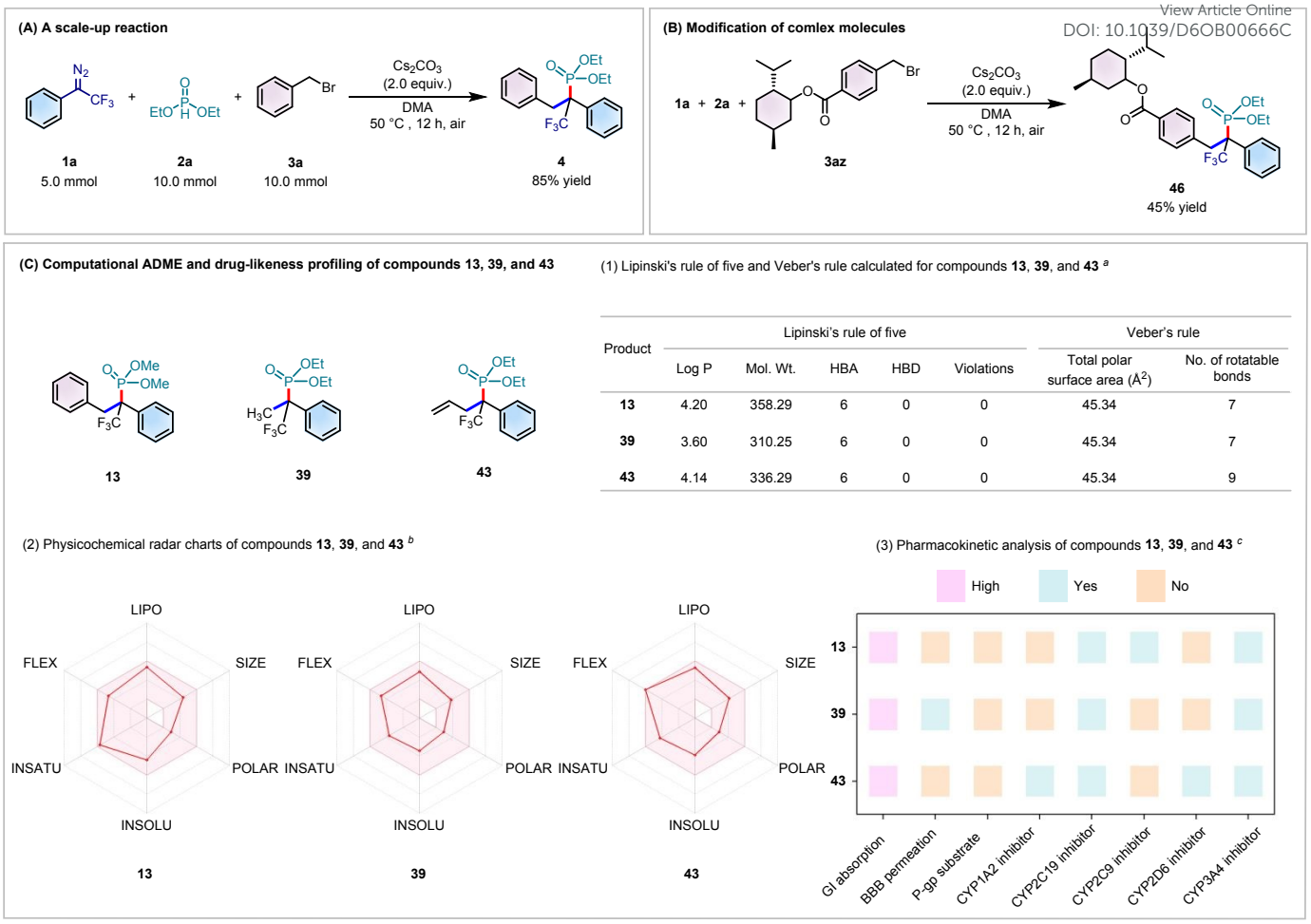

Product	Lipinski's rule of five					Veber's rule	
	Log P	Mol. Wt.	HBA	HBD	Violations	Total polar surface area (Å^2)	No. of rotatable bonds
13	4.20	358.29	6	0	0	45.34	7
39	3.60	310.25	6	0	0	45.34	7
43	4.14	336.29	6	0	0	45.34	9

Fig. 4. Synthetic applications and evaluation of pharmacokinetic profiles.[a] Mol. Wt.: molecular weight, HBA: hydrogen bond acceptors, HBD: hydrogen bond donors.[b] LIPO (Lipophilicity): -0.7<XLOGP3<+5.0, SIZE: 150g/mol<MV<500g/mol, POLAR (Polarity): 20Å^2<TPSA<130Å^2, INSOLU (Insolubility): 0<LogS (ESOL)<6, INSATU (Insaturation): 0.25<Fraction Csp^3<1, FLEX (Flexibility): 0<Num. of rotatable bonds<9.[c] GI: gastrointestinal, BBB: blood brain barrier, P-gp: p-glycoprotein.

To further highlight the synthetic utility of this method, a scale-up reaction was carried out under the standard conditions using **1a** (0.93 g, 5.0 mmol), **2a** (1.38 g, 10.0 mmol), and **3a** (1.71 g, 10.0 mmol). The desired product **4** was isolated in 85% yield (1.64 g, 4.25 mmol), demonstrating the robustness of the protocol (Fig. 4A). The applicability of this transformation was further extended to the modification of structurally complex molecules. For example, a benzyl bromide derived from L-menthol participated effectively in the reaction, furnishing the corresponding product **46** in 45% yield under the standard conditions (Fig. 4B).

In drug screening, due to the limited throughput and high cost of traditional experimental methods, computational approaches have emerged as preliminary tools for the early prediction of ADME parameters, which may help prioritize compounds for subsequent experimental validation.[40] In this study, the drug-likeness and key pharmacokinetic parameters of selected compounds were computationally estimated using the SwissADME platform.[41] The screening results indicate that compounds **13**, **39**, and **43** satisfy both Lipinski's Rule of Five and Veber's criteria, indicating favorable drug-like properties with no violations of the established constraints (Fig. 4C, (1)).[42] This finding was corroborated by the physicochemical radar plot (Fig. 4C, (2)), in which all data points fell within the optimal region.

A subsequent in silico analysis of the pharmacokinetic behavior was conducted for these three compounds (Fig. 4C, (3)). All three were predicted to exhibit high gastrointestinal absorption, which imply favorable oral bioavailability, although this requires experimental confirmation. In terms of targeting, only compound **39** was anticipated to cross BBB, indicating its potential for CNS-targeted applications; in contrast, compounds **13** and **43** showed no BBB permeation, rendering them more suitable for peripheral targets.[43] Notably, none of the three compounds were predicted to be substrates of P-glycoprotein (P-gp), which could suggest a low risk of multidrug resistance.[44] Furthermore, an evaluation of the cytochrome P450 inhibition profile, a critical indicator for assessing the risk of metabolic drug–drug interactions, revealed that these compounds may

inhibit specific CYP isoforms. This finding underscores the need for close monitoring of potential drug–drug interactions in subsequent investigations.[45]

Conclusions

In summary, we have established a mild and operationally simple three-component protocol for the direct construction of α-trifluoromethylated phosphonates. Employing α-trifluoromethyl diazo compounds as key precursors together with readily accessible H-phosphites and benzyl bromides or alkyl halides, this metal-free strategy enables the efficient construction of sterically congested, fully substituted carbon centers in a single operational step. The method exhibits broad substrate tolerance, accommodating a wide array of electronically and structurally diverse coupling partners, and delivers over 40 examples with yields reaching up to 98%. Its synthetic utility is further underscored by successful gram-scale synthesis and the late-stage functionalization of a menthol-derived pharmacophore. Computational ADME profiling of selected derivatives revealed promising pharmacokinetic attributes. Collectively, this work not only provides a versatile and sustainable entry point to α-trifluoromethylated phosphonates, but also establishes a foundation for future endeavours. Ongoing efforts in our laboratory are directed toward developing an asymmetric variant of this transformation and exploring its application in the construction of drug-like lead compounds.

Author contributions

A. Abdukader, L. Gong and G. Tang proposed and supervised the project. S. Zhang and X. Wu carried out the synthesis, characterization and data collection. S. Zhang, A. Abdukader, Y.-M. Lin and S. Wu analysis the date. S. Zhang, L. Gong and G. Tang wrote the paper with edits from all authors. All the authors discussed the results and commented on the manuscript.

Conflicts of interest

There are no conflicts to declare.

Data availability

The data supporting this article have been included as part of the supplementary information (SI). Supplementary information: synthesis, supplementary data and procedures; appendix of NMR spectra of new compounds. See DOI: https://doi.org/xxxx.

Acknowledgements

We thank the National Natural Science Foundation of China (No. 22571265, 22571263, 22061040, 22561046), and the Xinjiang Provincial Natural Science Foundation of China (No. 2022E01069).

References

View Article Online
DOI: 10.1039/D6OB00666C

1 M. C. Mayorquín-Torres, A. Simoens, E. Bonneure and C. V. Stevens, Chem. Rev., 2024, 124, 7907–7975.
2 P. Bhanja, J. Na, T. Jing, J. Lin, T. Wakihara, A. Bhaumik and Y. Yamauchi, Chem. Mater., 2019, 31, 5343–5362.
3 S. S. Iremonger, J. Liang, R. Vaidhyanathan, I. Martens, G. K. H. Shimizu, T. D. Daff, M. Z. Aghaji, S. Yeganegi and T. K. Woo, J. Am. Chem. Soc., 2011, 133, 20048–20051.
4 B. M. Johnson, Y.-Z. Shu, X. Zhuo and N. A. Meanwell, J. Med. Chem., 2020, 63, 6315–6386.
5 J. Wang, M. Sánchez-Roselló, J. L. Aceña, C. del Pozo, A. E. Sorochinsky, S. Fustero, V. A. Soloshonok and H. Liu, Chem. Rev., 2014, 114, 2432–2506.
6 T. Liang, C. N. Neumann and T. Ritter, Angew. Chem. Int. Ed., 2013, 52, 8214–8264.
7 K. D. Demadis, S. K. Adla, J. Timonen and P. A. Turhanen, Green Chem., 2025, 27, 863–914.
8 K. M. Heidel and C. S. Dowd, Future Med. Chem., 2019, 11, 1625–1643.
9 V. D. Romanenko and V. P. Kukhar, Chem. Rev., 2006, 106, 3868–3935.
10 Y. Zhou, J. Wang, Z. Gu, S. Wang, W. Zhu, J. L. Aceña, V. A. Soloshonok, K. Izawa and H. Liu, Chem. Rev., 2016, 116, 422–518.
11 A. Mucha, P. Kafarski and Ł. Berlicki, J. Med. Chem., 2011, 54, 5955–5980.
12 D. O'Hagan, Chem. Soc. Rev., 2008, 37, 308–319.
13 Y. Kondo, Y. Hirazawa, T. Kadota, K. Yamada, K. Morisaki, H. Morimoto and T. Ohshima, Org. Lett., 2022, 24, 6594–6598.
14 C. Liu, Y. Zhang, Q. Qian, D. Yuan and Y. Yao, Org. Lett., 2014, 16, 6172–6175.
15 P. Li, M. Jiang and J.-T. Liu, Chin. J. Chem., 2014, 32, 1003–1006.
16 X. Zhou, Q. Zhang, Y. Hui, W. Chen, J. Jiang, L. Lin, X. Liu and X. Feng, Org. Lett., 2010, 12, 4296–4299.
17 W.-Z. Fu, Y. Huang, X.-H. Xu and F.-L. Qing, Synth. Commun., 2016, 46, 415–420.
18 K. Yamada, Y. Kondo, A. Kitamura, T. Kadota, H. Morimoto and T. Ohshima, ACS Catal., 2023, 13, 3158–3163.
19 V. Krishnamurti, C. Barrett and G. K. S. Prakash, Org. Lett., 2019, 21, 1526–1529.
20 Z. Zhang and V. Gevorgyan, Chem. Rev., 2024, 124, 7214–7261.
21 Y.-L. Su, G.-X. Liu, L. De Angelis, R. He, A. Al-Sayyed, K. S. Schanze, W.-H. Hu, H. Qiu and M. P. Doyle, ACS Catal., 2022, 12, 1357–1363.
22 Y.-L. Su, G.-X. Liu, J.-W. Liu, L. Tram, H. Qiu and M. P. Doyle, J. Am. Chem. Soc., 2020, 142, 13846–13855.
23 D. P. Hari and J. Waser, J. Am. Chem. Soc., 2017, 139, 8420–8423.
24 M. Marinozzi, F. Pertusati and M. Serpi, Chem. Rev., 2016, 116, 13991–14055.
25 F. Zhao, H. Ding, T. Sun, C. Shen, Z.-L. Wang, W. Wei and D. Yi, Chin. Chem. Lett., 2026, 37, 111834.
26 H.-M. Lin, K. Li, X.-T. Li, X.-C. Liu, F. Yang, F.-H. Cui, H.-T. Tang, Y.-M. Pan and Y.-M. Lin, ACS Catal., 2026, 16, 228–241.
27 D. Hu, C. Pi, Y. Li, Y. Wu and X. Cui, Org. Lett., 2026, 28, 3298–3302.
28 D. Kumar, D. Chaudhary, K. Ishu, S. Yadav, N. K. Maurya, R. Kant and M. R. Kuram, Org. Biomol. Chem., 2022, 20, 8610–8614.
29 E. Levashova, M. Adamchik, D. Nikolaev, M. Ryazantsev and D. Dar'in, J. Org. Chem., 2024, 89, 16721–16735.
30 E. Levashova, M. Adamchik, I. Tatarinov and D. Dar'in, J. Org. Chem., 2026, 91, 2951–2964.
31 D. Chaudhary and M. R. Kuram, J. Org. Chem., 2024, 89, 7347–7351.
32 J.-L. Zhang, J.-X. Xiong, L.-Q. Fei, F.-H. Cui, S.-H. Li, H.-T. Tang, Y.-Z. Xie and Y.-M. Pan, Org. Chem. Front., 2024, 11, 3485–3490.

View Article Online
DOI: 10.1039/D6OB00666C

33 M. Gao, Y. Li, L. Xie, R. Chauvin and X. Cui, Chem. Commun., 2016, 52, 2846–2849.
34 Y. Zi, B. Yang, Z. Ye, Y.-M. Lin, Q. Zhao, B. Wang and L. Gong, Angew. Chem. Int. Ed., 2026, 65, e21100.
35 X. Cheng, T. Xu, T. Huang, G. Tang, Y.-M. Lin and L. Gong, J. Am. Chem. Soc., 2026, 148, 857–868.
36 F. Yang, L. Chi, Z. Ye and L. Gong, J. Am. Chem. Soc., 2025, 147, 1767–1780.
37 J. Cai, Y. Li, Z. Ye, W. Wang, Y. M. Lin and L. Gong, Green Synth. Catal., 2023, 4, 253–257.
38 S. Cao, Z. Ye, Y. Chen, Y.-M. Lin, J. Fang, Y. Wang, B. Yang and L. Gong, CCS Chem., 2021, 4, 3122–3133.
39 A. Daina, O. Michielin and V. Zoete, Sci. Rep., 2017, 7, 42717.
40 S. Ito, T. Koyama, S. Matsumoto, R. Kojima, Y. Okamoto, M. Kuroda, H. Kawashima, R. Watanabe, T. Yonezawa, T. Sumiyoshi, K. Ikeda, K. Mizuguchi, H. Iwata and Y. Okuno, J. Chem. Inf. Model., 2025, 65, 11796–11803.
41 K. Shah, S. Panchal and B. Patel, Pharmacol. Res., 2021, 167, 105532.
42 M. S. Alam and D.-U. Lee, Arch. Pharmacal Res., 2016, 39, 191–201.
43 A. C. Correia, A. R. Monteiro, R. Silva, J. N. Moreira, J. M. Sousa Lobo and A. C. Silva, Adv. Drug Delivery Rev., 2022, 189, 114485.
44 C.-P. Liu, C.-Y. Xie, J.-X. Zhao, K.-L. Ji, X.-X. Lei, H. Sun, L.-G. Lou and J.-M. Yue, J. Am. Chem. Soc., 2019, 141, 6812–6816.
45 J. Wu, X. Guan, Z. Dai, R. He, X. Ding, L. Yang and G. Ge, Coord. Chem. Rev., 2021, 427, 213600.

View Article Online
DOI: 10.1039/D6OB00666C

Data availability

The data underlying this study are available in the published article and its supplementary information (SI). The SI includes: general information, synthesis of substrates, three-component reactions, reaction optimization details, substrate scope studies, mechanistic experiments, synthetic utility, and characterization data for all products (**4**–**43**).

For further details, see DOI: https://doi.org/xxx/xxxxx.